ACADEMIC PRESS

Available online at www.sciencedirect.com

SCIENCE DIRECT®

DEVELOPMENTAL BIOLOGY

Developmental Biology 257 (2003) 205–219

www.elsevier.com/locate/ydbio

# Stem cell-derived endothelial cells/progenitors migrate and pattern in the embryo using the VEGF signaling pathway

Carrie A. Ambler,[a] Gayle M. Schmunk,[a] and Victoria L. Bautch[a,b,*]

[a] *Department of Biology, University of North Carolina at Chapel Hill, Chapel Hill, NC 27599, USA*
[b] *Carolina Cardiovascular Center, University of North Carolina at Chapel Hill, Chapel Hill, NC 27599, USA*

Received for publication 3 October 2002, revised 17 December 2002, accepted 7 January 2003

**Abstract**

Endothelial precursor cells respond to molecular cues to migrate and assemble into embryonic blood vessels, but the signaling pathways involved in vascular patterning are not well understood. We recently showed that avian vascular patterning cues are recognized by mammalian angioblasts derived from somitic mesoderm through analysis of mouse–avian chimeras. To determine whether stem cell-derived endothelial cells/progenitors also recognize global patterning signals, murine ES cell-derived embryoid bodies (EBs) were grafted into avian hosts. ES cell-derived murine endothelial cells/progenitors migrated extensively and colonized the appropriate host vascular beds. They also formed mosaic vessels with avian endothelial cells. Unlike somite derived-endothelial cells, ES cell-derived endothelial cells/progenitors migrated across the host embryonic midline to the contralateral side. To determine the role of VEGF signaling in embryonic vascular patterning, EBs mutant for a VEGF receptor (*flk-1*$^{-/-}$) or a signal (*VEGF-A*$^{-/-}$) were grafted into quail hosts. *Flk-1*$^{-/-}$ EB grafts produced only rare endothelial cells that did not migrate or assemble into vessels. In contrast, *VEGF-A*$^{-/-}$ EB grafts produced endothelial cells that resembled wild-type and colonized host vascular beds, suggesting that host-derived signals can partially rescue mutant graft vascular patterning. *VEGF-A*$^{-/-}$ graft endothelial cells/progenitors crossed the host midline with much lower frequency than wild-type EB grafts, indicating that graft-derived VEGF compromised the midline barrier when present. Thus, ES cell-derived endothelial cells/progenitors respond appropriately to global vascular patterning cues, and they require the VEGF signaling pathway to pattern properly. Moreover, EB–avian chimeras provide an efficient way to screen mutations for vascular patterning defects.


*Keywords:* Vascular pattern; Blood vessel formation; ES cells; In vitro differentiation; Avian chimeras; Murine graft; VEGF signaling; flk-1; VEGF-A

## Introduction

Early elegant descriptions of vascular development (Sabin, 1917; Clark and Clark, 1939) resulted in a model of blood vessel formation that is still useful today (reviewed in Poole and Coffin, 1989; Risau, 1997; Drake et al., 1998; Daniel and Abrahamson, 2000). Blood vessels form developmentally by two processes—vasculogenesis and angiogenesis. Vasculogenesis is the coalescence and differentiation of mesodermal precursor cells to form vessels, and angiogenesis involves the migration and division of already differentiated endothelial cells to form new vasculature. This primary vascular plexus is then remodeled by interactions between endothelial cells and other mesodermal cells, primarily smooth muscle cells and pericytes (Orlidge and D'Amore, 1987). These processes are coordinated with other developmental events by vascular patterning cues that instruct blood vessels where and when to form.

The cellular and molecular processes that control vascular patterning are largely unknown. Genetic analyses in mice and zebrafish suggest that the Notch, ephrin, and EDG pathways, as well as unidentified genes such as *out-of-bounds*, are involved in patterning the primary vascular plexus (reviewed in Hogan and Kolodziej, 2002) (Pereria et al., 1999; Zhong et al., 2000; Graef et al., 2001; Childs et al., 2002). Unfortunately, the early lethality of mice carrying VEGF pathway mutations has prevented rigorous genetic evaluation of VEGF signaling in mammalian vascular

* Corresponding author. Fax: +1-919-962-8472.
*E-mail address:* bautch@med.unc.edu (V.L. Bautch).

0012-1606/03/$ – see front matter © 2003 Elsevier Science (USA). All rights reserved.
doi:10.1016/S0012-1606(03)00042-3

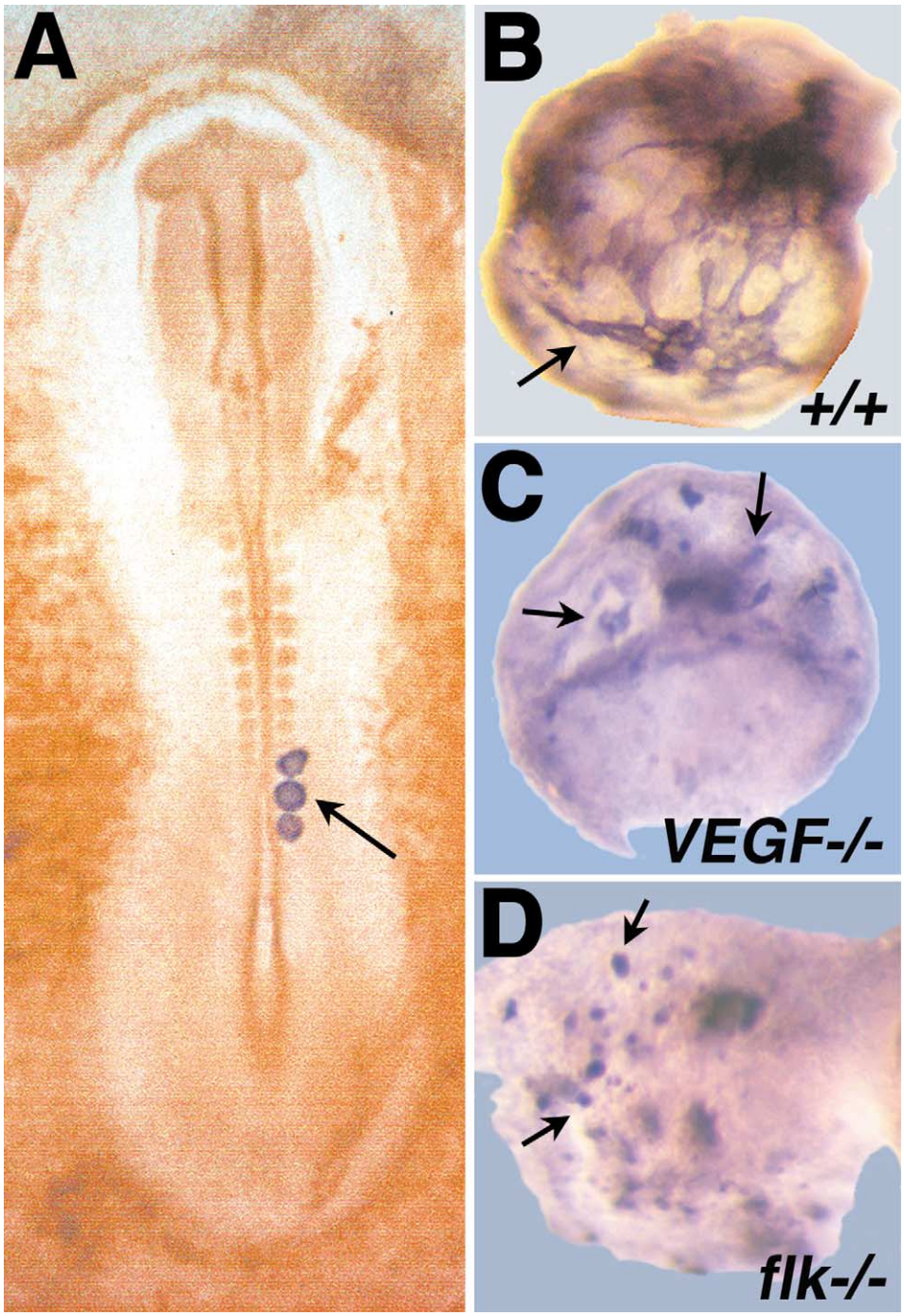


Fig. 1. Mouse embryoid body (EB) placement in an avian host and in vitro differentiation. (A) Day 3–4 murine EBs were labeled with Nile Blue, then placed on one side of the presomitic mesoderm cavity of an 11-somite (HH stage 10+) quail host and photographed *in ovo*. Arrow points to EBs and the graft site. (B–D) EBs of different genotypes were allowed to differentiate in vitro to day 7 (analogous to the age of EBs in grafts when analyzed), then stained for PECAM-1 in whole mount. (B) Wild-type EB; (C) *VEGF-A*$^{-/-}$ EB; (D) *flk-1*$^{-/-}$ EB. The arrow in (B) points to the vascular plexus, while in (C) and (D), the arrows point to PECAM-positive clumps of angioblasts.

patterning. However, endothelial cells have morphogenetic properties that are regulated by VEGF, suggesting involvement in vascular patterning. Moreover, several studies firmly link VEGF expression by astrocytes and neurons to local vessel patterning in the retina and limb (Stone et al., 1995; Zhang et al., 1999; Mukuoyama et al., 2002; Otani et al., 2002).

Embryological approaches have provided clues to vascular patterning constraints in the embryo. The seminal work of Noden established that avian angioblasts are highly

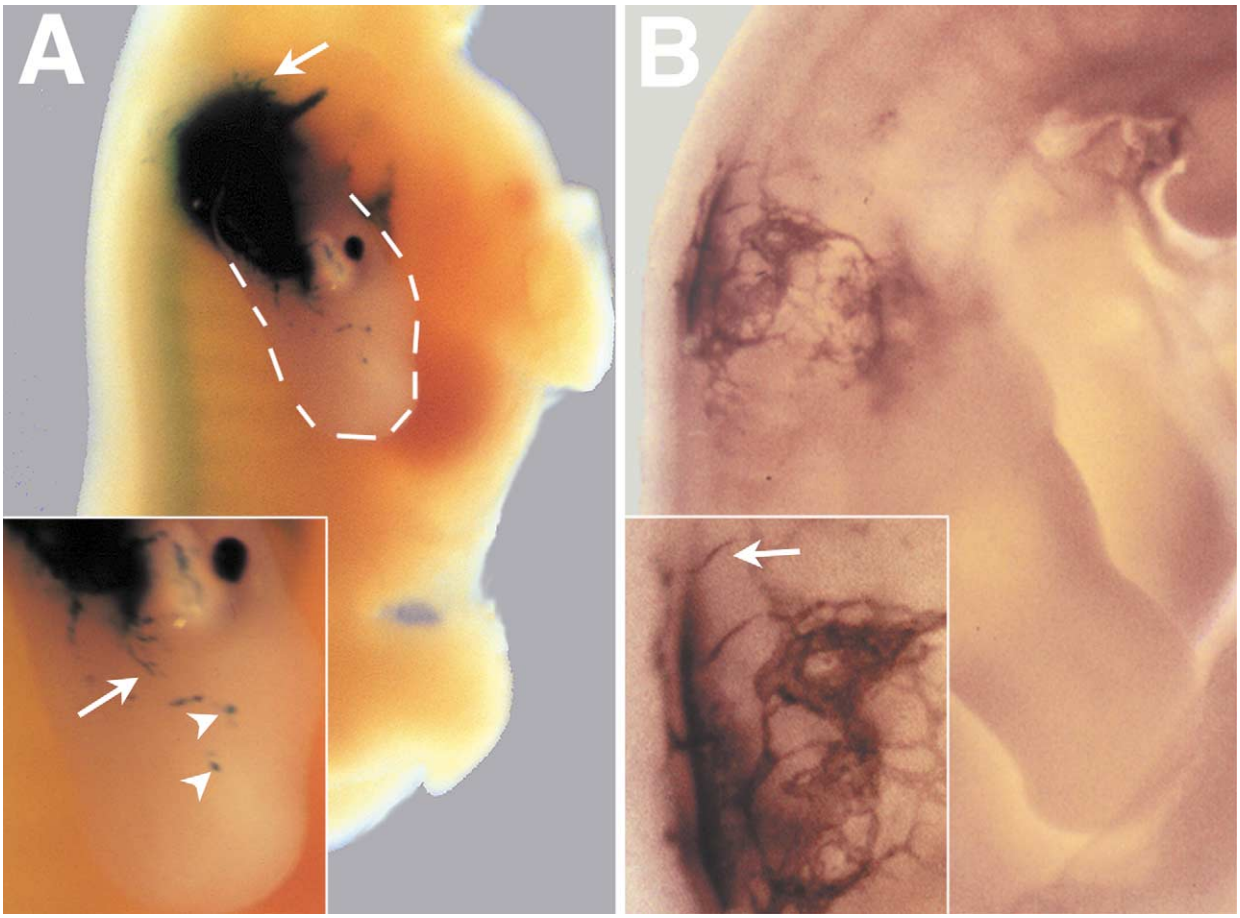


Fig. 2. EB grafts incorporate and produce vasculature in avian hosts. Day 3 EBs were placed in quail hosts as in Fig. 1, then incubated *in ovo* for 3–4 additional days. (A) *ROSA26*$^{+/-}$ (wild-type) EB–avian chimera whole mount stained for β-gal reactivity (blue). Day 4 EBs were placed into a 14-somite (HH stage 11+) host and incubated for 3 days, to HH stage 24. The dashed line outlines the limb, and the arrow points to β-gal-positive graft tissue. The inset is a higher magnification of the same graft. The arrow points to extensions from the graft proper that resemble blood vessels, and the arrowheads point to small clumps of graft cells that are distinct from the graft body. (B) Wild-type EB-avian chimera whole mount stained for PECAM (purple) to visualize graft-derived vasculature. Day 3 EBs were placed into a 19-somite (HH stage 13) host and incubated for 3 days, to HH stage 25. The inset is a higher magnification of the same graft. The arrow points to a graft-derived vessel in the vertebral area of the quail host.

migratory and originate from most embryonic tissues (Noden, 1989). Subsequent work using quail-chick chimeras showed that: (1) avian somites are a source of angioblasts that migrate extensively and colonize vascular beds of the trunk and limb; and (2) avian angioblasts are restricted from crossing the axial midline and colonizing the contralateral side of the embryo (Wilting et al., 1995; Pardanaud et al., 1996). We recently extended these results to mammalian vascular cells using mouse–avian chimeras, and we showed that mouse somite-derived angioblasts respond to avian patterning signals (Ambler et al., 2001).

The recent interest in stem cells as a possible source of endothelial cells capable of providing therapeutic relief led us to consider whether ES cell-derived endothelial cells and/or their progenitors (endothelial cells/progenitors) could respond to vascular pattern cues. Here, we demonstrate that ES cell-derived endothelial cells/progenitors migrate and pattern in response to embryonic vascular patterning signals. Genetic dissection of VEGF signaling in this process revealed a critical role for the VEGF receptor flk-1. The VEGF-A ligand was also important, but host-derived signals could partially rescue *VEGF-A*$^{-/-}$ endothelial cell patterning. Our novel use of ES cell-derived embryoid body grafts in avian hosts should provide an efficient way to screen mutations for vascular patterning defects.

## Materials and methods

### *ES cells*

R1, ROSA (*ROSA26*$^{+/-}$), flt-1 hemizygous (*flt-1*$^{+/-}$), flk-1 hemizygous (*flk-1*$^{+/-}$) VEGF mutant (*VEGF-A*$^{-/-}$), and homozygous flk-1 mutant (*flk-1*$^{-/-}$) ES cells were cultured and differentiated into embryoid bodies (EBs) as previously described (Wang et al., 1992; Bautch, 2002). At day

3 or 4 of differentiation, EBs were implanted into avian hosts. Some EBs were cultured for an additional 3-4 days (to day 6 or 7 of differentiation) prior to fixation.

### *Chimeras*

Fertilized Japanese quail eggs (CBT Farms, Chestertown, MD) were incubated at 37°C for 2 days prior to surgery. The HH 10 stage (Hamburger and Hamilton, 1951) quail hosts were prepared in ovo. The vitelline membrane was peeled back, and the quail presomitic mesoderm was removed by using sharpened tungsten needles.

Day 3 or 4 EBs were removed from tissue culture medium and rinsed in Ringer's solution. EBs were then labeled with 1% Nile Blue (Sigma) by using a glass needle, and one to three EBs were positioned within the cavity of the host made by removal of the presomitic mesoderm. The chimeric embryos were sealed with Parafilm and allowed to incubate for 3 or 4 days at 37°C in a humidified incubator. For time course experiments, EBs were incubated with 0.2 ng/ml CM-Dil (Molecular Probes, Eugene, OR) added to the culture medium during culture in vitro. EBs were incubated in 200 ng/ml CM-Dil in PBS for 5 min immediately prior to implantation. Chimeras were analyzed at 18, 24, or 36 h postsurgery as described below, and fluorescence was visualized with an Olympus IX 50 inverted microscope.

### *β-Galactosidase detection and immunohistochemistry*

Embryos were processed for whole-mount β-galactosidase detection and immunohistochemistry as previously described (Ambler et al., 2001). Briefly, for β-galactosidase detection (adapted from Beddington et al., 1989), embryos were sacrificed 3 or 4 days postsurgery, rinsed in PBS, and fixed in 4% paraformaldehyde (PFA) for 20 min at room temperature. Chimeras were washed two times for 10 min in wash buffer [0.1 M phosphate buffer (pH 7.3), 0.1% sodium desoxycholate, 0.02% NP40, 0.05% BSA (Sigma)], then transferred to wash buffer containing 1 mg/ml X-gal (Sigma), 5 mM ferrocyanide, and 5 mM ferricyanide. After incubation for 14–18 h at 37°C in the dark, embryos were postfixed in 4% PFA and stored at 4°C until embedded.

For whole-mount immunohistochemistry (adapted from Dent et al., 1989), chimeric embryos were fixed for 24–72 h in 4% PFA at 4°C, dehydrated through a MeOH series, and stored in 100% MeOH at −20°C. They were exposed to 3% $H_2O_2$/MeOH overnight at 4°C, followed by rehydration to PBS. Embryos were incubated for 10 min in a solution of 1 μg/ml proteinase K (Sigma) in 50 mM Tris (pH 8.0)/5 mM EDTA, and washed for 5 min in 2 mg/ml glycine in PBS/0.1% Tween 20 (PBT). After blocking overnight at 4°C in TBSTN [Tris-buffered saline (pH 7.5)/0.05% Tween 20 (TBST)/20% heat-inactivated FCS], the chimeric embryos were incubated overnight at 4°C with rat anti-mouse PECAM (MEC 13.3; BD Pharmingen) at 1:200 in TBSTN. Five 1-h washes in TBST were followed by addition of HRP-conjugated goat anti-rat secondary antibody (Pierce) at 1:200 in TBSTN. After incubation overnight at 4°C, embryos were washed five times for 1 h each in TBST at room temperature followed by an overnight wash in TBST at 4°C. The antibody was detected by incubation in PBS/0.5 mg/ml DAB (Sigma)/0.03% $H_2O_2$/3 mg/ml $NiSO_4$ for 30 min, resulting in a purple reaction product. Sometimes the $NiSO_4$ was eliminated to yield a brown reaction product.

For whole-mount immunohistochemical staining of embryoid bodies (EBs), they were fixed, dehydrated, and stored as described for chimeric embryos. EBs were rehydrated in a MeOH/PBS series, exposed to 1 M glycine/PBS for 30 min, followed by two 15-min washes in PBS, then treated with 6% $H_2O_2$/PBS for 25 min. They were rinsed in PBT two times for 15 min, then permeabilized with 10 μg/ml proteinase K (Sigma) in PBS for 3 min, followed by 2 mg/ml glycine in PBT for 5 min. After washing three times for 5 min in PBT, EBs were blocked in PBT/5% heat-inactivated FCS (PBTN) for 30 min at room temperature. They were incubated overnight at 4°C with rat anti-mouse PECAM (MEC 13.3) at 1:200 in PBTN. EBs were washed for 2 h in PBT, then incubated overnight at 4°C with an HRP-conjugated goat anti-rat secondary antibody at 1:200 in PBTN. After the overnight incubation, EBs were rinsed in PBT for 2 h. Detection was by incubation in PBS/0.33 mg/ml DAB (Sigma)/0.006% $H_2O_2$/3 mg/ml $NiSO_4$ for 5 min, resulting in a purple reaction product. EBs were rinsed and stored in PBS until photographed. Chimeric embryos and EBs were visualized and photographed with an Olympus SZH10 dissecting microscope.

Embryos were embedded and sectioned as previously described (Ambler et al., 2001). Briefly, embryos were dehydrated through a MeOH series and then transferred to 100% EtOH for 20 min. The embryos were incubated in 50% EtOH/xylenes, 100% xylenes, 50% xylenes/50% paraffin for 30 min each, then incubated with melted paraffin at 58°C for 24–48 h. The paraffin was solidified at room temperature, and 12-μm transverse sections were cut on a microtome.

For QH1 staining, dried sections were cleared in Histoclear (National Diagnostics) before rehydrating through an EtOH series. Slides were rinsed in PBS, then exposed to 0.23% $H_2O_2$/PBS for 15 min. Slides were incubated overnight at 4°C with a 1:200 dilution of QH1 (Developmental Studies Hybridoma Bank, Iowa City, IA) in PBS/5% goat serum. Slides were rinsed in PBS for 15–20 min followed by a 2-h incubation of HRP-conjugated goat anti-mouse IgG (Jackson ImmunoResearch) in PBS/5% goat serum and a DAB/$H_2O_2$ reaction as described for staining of chimeric embryos. Slides were mounted with Glycergel (Dako) and visualized with a Nikon Opitphot 2 microscope.

## Results

### *Stem cell-derived endothelial cells/progenitors migrate and pattern properly in the avian host*

Differentiation of murine ES cells in vitro leads to a programmed differentiation of several cell types, including endothelial cells. We took advantage of this model to assess the behavior of ES cell-derived murine endothelial cells and/or their progenitor cells (endothelial cells/progenitors) when grafted into an avian host. Partially differentiated EBs at days 3–4 of differentiation contain endothelial precursor cells called angioblasts, but few if any mature endothelial cells (Yamashita et al., 2000). One to three EBs were placed into appropriately staged quail embryos, in a cavity made by removal of the presomitic mesoderm from one side of the neural tube (Fig. 1A). Companion EBs from the same differentiation were incubated for an additional 3–4 days in culture to determine their capacity to differentiate and form primitive vessels in vitro (Fig. 1B–D). Mouse endothelial cells and at least a subset of angioblasts express the vascular marker PECAM (Baldwin et al., 1994; Redick and Bautch, 1999; Bautch et al., 2000). Wild-type EBs formed in vitro had an extensive PECAM$^{+}$ primitive vasculature (Fig. 1B), while *VEGF-A*$^{-/-}$ EBs and *flk-1*$^{-/-}$ EBs had rare clumps of PECAM$^{+}$ angioblasts, but no extensive vasculature (Fig. 1C and D). These results were expected because vascular development peaks at days 7–8 of ES cell differentiation and is dependent on the VEGF signaling pathway (Wang et al., 1992; Vittet et al., 1996; Shalaby et al., 1997; Fong et al., 1999; Bautch et al., 2000; Kearney et al., 2002).

After 3 days of incubation in the quail host, *ROSA26*$^{+/-}$ EBs that constitutively express $\beta$-galactosidase ($\beta$-gal) showed extensive colonization of the quail embryo (Fig. 2A). Moreover, $\beta$-gal-positive murine graft cells were seen at some distance from the main body of the graft, and $\beta$-gal-positive structures with vessel morphology were seen adjacent to the main body of the graft (inset, Fig. 2A). Transverse sections of the *ROSA26*$^{+/-}$ EB-chimeric embryos showed graft survival and placement in the somitic area, with extensive migration of graft-derived cells (Fig. 3A). Some of these cells were associated with QH1-positive quail host vessels (Pardanaud et al., 1987), suggesting that they were ES cell-derived endothelial cells.

Wild-type EBs (+/+) were grafted and incubated as described above, and the chimeric embryos were stained in whole mount for PECAM reactivity, since this marker of mouse endothelial cells does not cross-react with quail vascular cells (Ambler et al., 2001). The PECAM staining pattern showed extensive murine ES cell-derived vessels at the graft site and adjacent to it (Fig. 2B). Thus ES cell-derived endothelial cells can differentiate and assemble into vessels in the avian host. The pattern of PECAM-1$^{+}$ vessels dorsal to the graft site suggested that graft-derived endothelial cells contributed to host vascular beds in the intersomitic and vertebral areas (inset, Fig. 2B).

A second group of grafts was generated by using EBs that were hemizygous for the VEGF receptor flt-1 (*flt-1*$^{+/-}$), expressing the *lacZ* reporter gene under control of the flt-1 promoter (Fong et al., 1995). In these EBs, $\beta$-gal is expressed in cells that express flt-1, which include murine angioblasts and endothelial cells, and there is no detectable phenotype resulting from hemizygosity at the *flt-1* locus (Fong et al., 1996; Kearney et al., 2002). Analysis of transverse sections of the *flt-1*$^{+/-}$ EB-chimeric embryos counterstained with QH1 showed that ES-cell derived endothelial cells/progenitors migrated from the graft site and contributed to host vascular beds (Fig. 3B–D). For example, $\beta$-gal and QH1 staining was colocalized in the intersomitic area (Fig. 3B), the kidney rudiment (Fig. 3B), the limb (Fig. 3C), and the perineural area (Fig. 3D) of the quail host.

These sites of ES cell-derived endothelial cell colonization corresponded to sites of colonization of presomitic mesoderm-derived murine endothelial cells (Ambler et al., 2001), suggesting that ES cell-derived endothelial cells/progenitors respond to similar patterning cues in the avian host. To obtain quantitative data, chimeric embryos containing wild-type (+/+) and *ROSA26*$^{+/-}$ EB grafts, and *flt-1*$^{+/-}$ EB grafts, were serially sectioned in the transverse plane, counterstained with QH1, and examined throughout the trunk region. Graft cell contribution to the host vascular beds described above was scored and compared with a similar quantitation of presomitic mesoderm-derived grafts (Ambler et al., 2001). The results are shown in Table 1. They indicate that ES cell-derived endothelial cells are similar to embryonic endothelial cells from the presomitic mesoderm in contributing extensively to the host intersomitic, limb, kidney, and perineural vascular beds. Minor differences include slightly lower frequencies of contribution to the perineural (82 vs. 100%) and kidney (70 vs. 100%) vascular beds by ES cell-derived endothelial cells.

The ability of ES cell-derived endothelial cells/progenitors to cross the embryonic midline and colonize the contralateral side of the host was also scored. In contrast to presomitic mesoderm-derived vascular cells that never crossed the host midline, the ES cell-derived endothelial cells/progenitors crossed the midline 35% of the time (Fig. 3E, and Table 1). In the majority of cases, the ES cell-derived endothelial cells were found exclusively in the intersomitic vascular region on the contralateral side of the host (Fig. 3E), and in rare instances, they also colonized the contralateral perineural area (data not shown). However, ES cell-derived endothelial cells were never seen in the contralateral limb or kidney vascular beds, suggesting that migration on the contralateral side was limited. The ability of nonvascular ES cell-derived graft cells to cross the host midline was not scored in these experiments.

To examine in more detail the relationship of ES cell-derived murine endothelial cells and quail endothelial cells, sections of chimeric embryos that carried grafts from wild-type (+/+) or *flt-1*$^{+/-}$ EBs that have a wild-type phenotype were examined at higher magnification (Fig. 4). Numerous

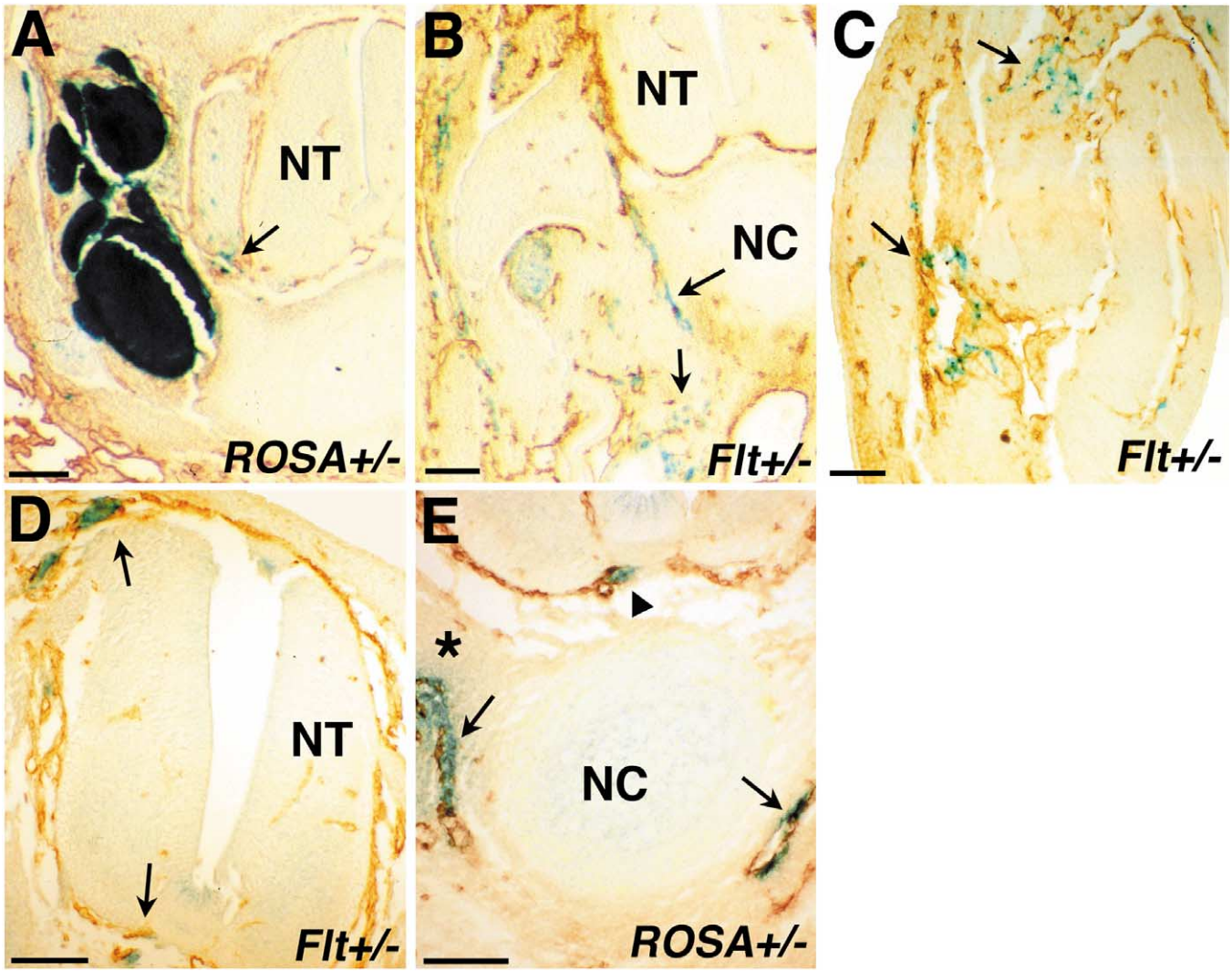


Fig. 3. ES cell-derived endothelial cells/progenitors migrate and pattern in avian hosts. EB–avian chimeras made with either *ROSA*$^{+/-}$ (A, E) or *flt-1*$^{+/-}$ (B–D) EBs that have a wild-type phenotype were whole-mount stained for $\beta$-gal (blue) reactivity to visualize graft-derived cells (ROSA) or endothelial cells (flt-1), and transverse sections were then counterstained with QH1 (brown) to visualize host blood vessels. (A) *ROSA*$^{+/-}$ EB graft showing graft incorporation into the somitic region of the host. Day 3 EBs were placed into a 15 somite (HH stage 12+) host, and incubated for 4 days, to HH stage 25. The large area of blue cells adjacent to the neural tube is graft tissue. The arrow points to graft-derived cells that appear to have migrated from the graft site and associate with QH1-positive host vessels in the perineural area. (B) *Flt*$^{+/-}$ EB graft showing graft endothelial cells in several midline host vascular beds. Day 4 EBs were placed into a 13-somite (HH stage 11) host, and incubated for 3 days, to HH stage 24. The arrows point to several of numerous areas where graft-derived endothelial cells are found associated with QH1-positive host vessels. The upper arrow points to a mosaic vessel in the intersomitic area, and the lower arrow points to graft-derived endothelial cells in the kidney rudiment of the host. (C) *Flt*$^{+/-}$ EB graft showing graft endothelial cells in the limb. Day 4 EBs were placed into a 13-somite (HH stage 11) host, and incubated for 3 days, to HH stage 24. The arrows point to two distinct regions where graft-derived endothelial cells appear to form mosaic vessels with host endothelial cells. (D) *Flt*$^{+/-}$ EB graft showing graft endothelial cells in the perineural area. Day 4 EBs were placed into an 11-somite (HH stage 10+) host, and incubated for 3 days, to HH stage 24. The arrows point to two distinct perineural regions where graft-derived endothelial cells are associated with host endothelial cells. (E) *ROSA*$^{+/-}$ EB graft showing midline crossing of graft-derived cells. Day 4 EBs were placed into a 10-somite (HH stage 10) host, and incubated for 3 days, to HH stage 24. The asterisk indicates the graft side of the host. The arrow below the asterisk points to graft-derived cells associated with host intersomitic vessels on the graft side, while the arrow on the opposite side points to graft-derived cells associated with host intersomitic vessels on the contralateral side. The arrowhead points to graft-derived cells in the perineural area on the graft side of the host. NC, notochord; NT, neural tube. Scale bars, 50 $\mu$m.

instances of apposition between host and graft vascular cells were noted. For example, a small PECAM$^+$ graft vessel appeared embedded in a QH1$^+$ quail vessel, while nearby, a putative junction between graft and host endothelial cells was seen (Fig. 4A). In other cases, the graft vessels were closely apposed to but largely unlinked to host vessels (Fig. 4D). $\beta$-Gal-positive *flt-1*$^{+/-}$ graft endothelial cells also formed mosaic vessels (Fig. 4B and E) or were found in close apposition to host vessels (Fig. 4C) in several vascular beds. In rare instances, graft vessels had QH1$^+$ host cells in the vessel lumen with hematopoietic morphology. Since QH1 is also expressed on quail hematopoietic precursors

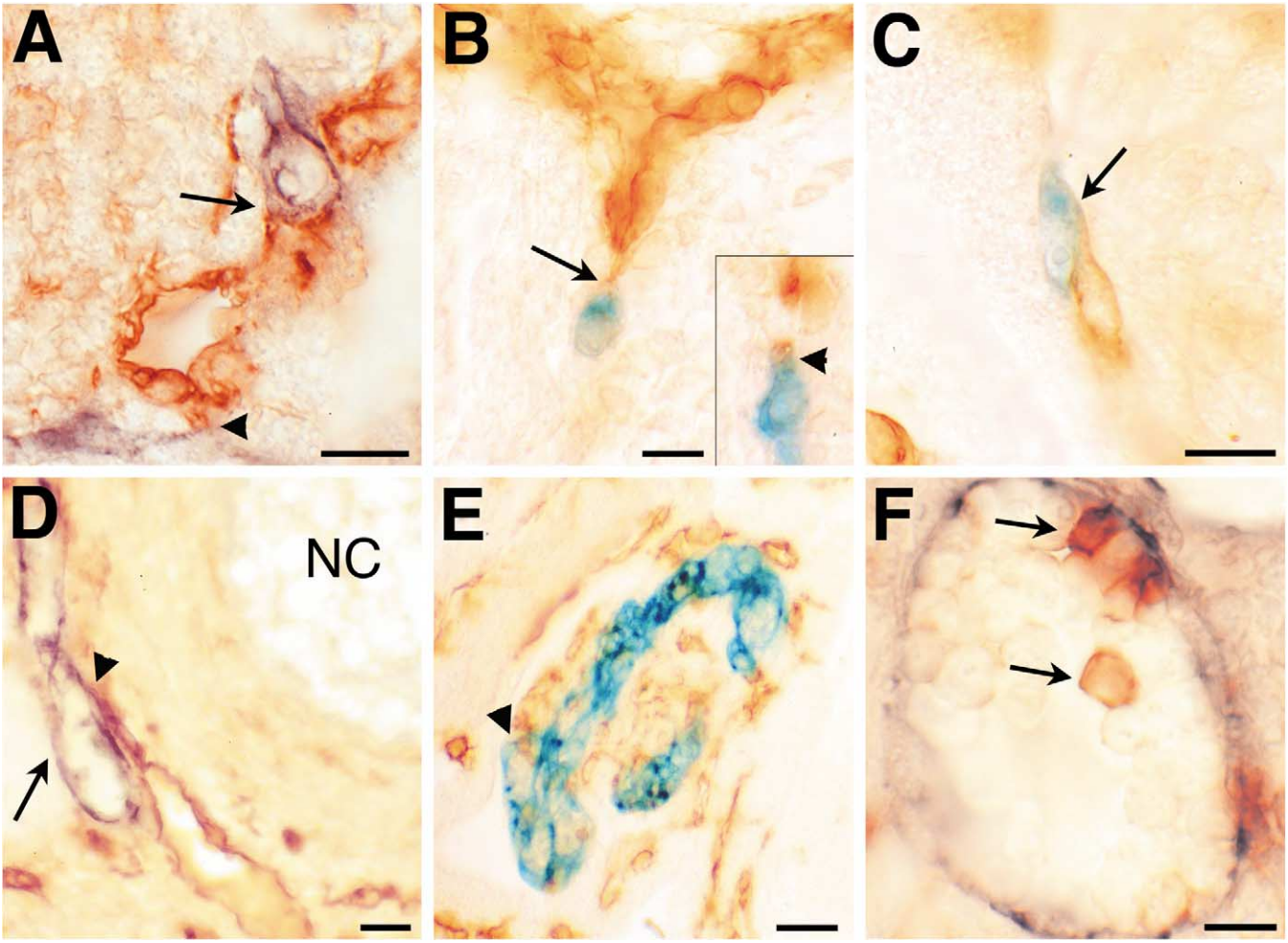


Fig. 4. ES cell-derived endothelial cells associate with and form mosaic vessels with avian host vessels. Higher magnification of transverse sections of EB–quail chimeras. (A, D, F) Wild-type EB grafts whole-mount stained for PECAM (purple). (B, C, E) *flt-1*$^{+/-}$ EB grafts whole-mount stained for $\beta$-gal (blue). In all panels, sections are counterstained with QH1 (brown) to visualize host endothelial cells. (A) Vascular bed in the limb. Day 4 EBs were placed into a 14-somite (HH stage 11+) host, and incubated for 3 days, to HH stage 24. The arrow points to a juxtaposition of graft and host vessels, and the arrowhead points to the area where graft and host vessels may have joined. (B) Quail intersomitic vessel with a small clump of graft-derived vascular cells at the distal tip. Day 4 EBs were placed into a 13-somite (HH stage 11) host, and incubated for 3 days, to HH stage 24. The arrow points to the juxtaposition of graft and host vascular cells. Inset, closeup of an adjacent section. The arrowhead points to what appears to be a junction between graft and host endothelial cells. (C) Vascular bed in the limb. Day 4 EBs were placed into a 17-somite (HH stage 12+) host, and incubated for 3 days, to HH stage 24. The arrow points to a graft-derived vessel that is in close apposition to the adjacent host vessel. (D) Vascular bed in the intersomitic region. Day 4 EBs were placed into an 11-somite (HH stage 10+) host, and incubated for 3 days, to HH stage 24. The arrow points to a graft-derived vessel that is in close apposition to the adjacent host vessel. The arrowhead points to an area where the graft and host vessels appear to have joined. (E) Vascular bed in the kidney rudiment. Day 4 EBs were placed into a 13-somite (HH stage 11) host, and incubated for 3 days, to HH stage 24. The arrowhead points to a junction in a mosaic vessel. (F) Vascular bed in the somitic cavity. Day 4 EBs were placed into a 17-somite (HH stage 12+) host, and incubated for 3 days, to HH stage 24. Arrows point to QH1 positive quail cells that appear hematopoietic by morphology and location within a graft-derived vessel. NC, notochord. Scale bars, 10 $\mu$m.

(Pardanaud et al., 1987), this finding suggests that ES cell-derived endothelial cells can form functional vessels and support blood flow.

To determine whether migrating vascular cells express endothelial lineage markers while migrating, we examined the temporal and spatial pattern of expression of flk-1, a marker of endothelial cells/progenitors. EBs that were hemizygous for the VEGF receptor flk-1 (*flk-1*$^{+/-}$), expressing the *lacZ* reporter gene under control of the flk-1 promoter (Shalaby et al., 1995), were analyzed at early times after surgery (Fig. 5). At 12 h postsurgery, no $\beta$-gal-positive cells were seen outside the graft boundaries, as determined by Dil labeling of the graft tissue prior to surgery (data not shown). However, at 18 h postsurgery and beyond, individual or small groups of $\beta$-gal-positive cells could be seen at sites outside the graft proper (Fig. 5A–F). Transverse sections of graft sites at 24 h postsurgery showed $\beta$-gal-positive cells both within the graft proper and outside the graft boundaries (Fig. 5G–L). Inspection of adjacent sections showed that the $\beta$-gal reactivity was confined to a single section, suggesting that these were single cells or very small clumps of cells in the process of migra-

Table 1
Location of mouse graft vascular cells in quail hosts at 72–96 h

| Graft type | Area containing graft endothelial cells | | | | |
|---|---|---|---|---|---|
| | Intersomitic | Perineural | Limb[b] | Kidney[b] | Contralateral side |
| WT PSM[a] | 76% (13/17) | 100% (17/17) | 83% (10/12) | 100% (17/17) | 0% (0/17) |
| WT EB | 82% (14/17) | 82% (14/17) | 70% (7/10) | 70% (7/10) | 35% (6/17) |
| *Flk-1*$^{-/-}$ EB | 0% (0/9) | 0% (0/9) | 0% (0/9) | 0% (0/9) | 0% (0/9) |
| *VEGF*$^{-/-}$ EB Type 1 | 100% (8/8) | 88% (7/8) | 86% (6/7) | 75% (3/4) | 13% (1/8) |
| *VEGF*$^{-/-}$ EB Type 2 | 0% (0/7) | 43% (3/7) | 20% (1/5) | 20% (1/5) | 0% (0/7) |

[a] Wild-type presomitic mesoderm grafts (from Ambler et al., 2001).
[b] Not all grafts were positioned to contribute to the limb and/or kidney areas.

tion. We also saw β-gal-negative graft-derived cells that had migrated from the original graft site (data not shown). In summary, the temporal and spatial expression of β-gal from the flk-1 locus of grafted EBs suggests that some migrating cells express flk-1, indicating that they are specified to the vascular lineage before or during migration.

### *The VEGF signaling pathway is required for patterning vessels at the embryonic midline*

The availability of ES cells lacking components of the VEGF signaling pathway allowed us to investigate how perturbations of this pathway affect embryonic vascular patterning. *Flk-1*$^{-/-}$ ES cells lack an essential VEGF receptor, and they form reduced numbers of angioblasts and only rare small vessels upon in vitro differentiation (Schuh et al., 1999) (Fig. 1D). *Flk-1*$^{-/-}$ EBs survived in quail hosts, and small numbers of PECAM$^{+}$ angioblasts were found in clumps (Fig. 6A and B; Fig. 7A and B). Although QH1$^{+}$ quail vessels were seen nearby, the *flk-1*$^{-/-}$ angioblasts did not form connections with quail endothelial cells or form mosaic vessels. Moreover, the rounded morphology of the *flk-1*$^{-/-}$ graft cells expressing PECAM suggested that they did not migrate from the graft upon differentiation. Analysis of serially sectioned grafts was consistent with a migration defect, since *flk-1*$^{-/-}$ graft endothelial cells were never seen in the host vascular beds colonized by wild-type murine endothelial cells (Table 1). Thus the VEGF receptor flk-1 is required for proper migration and patterning of ES cell-derived endothelial cells/progenitors.

*VEGF-A*$^{-/-}$ ES cells also produce reduced numbers of angioblasts and rare small vessels when differentiated in vitro (Bautch et al., 2000). In contrast, *VEGF-A*$^{-/-}$ EBs produced endothelial cells/progenitors that migrated and patterned in the avian host (Fig. 6C–E; Fig. 7C–F). The *VEGF-A*$^{-/-}$ EB grafts fell into two categories. Type 1 grafts were formed from small EBs, and these grafts produced an extensive graft-derived vasculature (Fig. 6C and D; Fig. 7C and D). Type 1 *VEGF-A*$^{-/-}$ endothelial cells formed mosaic vessels with wild-type quail endothelial cells (Fig. 7D, and inset), and they colonized host vascular beds at frequencies similar to those of wild-type ES cell-derived endothelial cells (Table 1). Type 2 *VEGF-A*$^{-/-}$ grafts were formed from larger EBs, and these grafts produced fewer graft-derived vessels and more clumps of PECAM$^{+}$ murine cells (Fig. 6E; Fig. 7E and F). However, in contrast to the *flk-1*$^{-/-}$ endothelial cells/progenitors, the *VEGF-A*$^{-/-}$ endothelial cells/progenitors from Type 2 grafts appeared to migrate to some extent (Fig. 7E, and Table 1), and they were often found immediately adjacent to quail vessels (Fig. 7F). Thus, in general, endothelial cells/progenitors derived from *VEGF-A*$^{-/-}$ EBs migrated and patterned properly in the quail hosts. The difference between Type 1 and Type 2 *VEGF-A*$^{-/-}$ grafts suggests that larger EBs are less amenable to rescue by signals from the quail host, perhaps because the host signals have difficulty penetrating to vascular cells in the larger EBs.

Interestingly, ES cell-derived endothelial cells/progenitors from *VEGF-A*$^{-/-}$ grafts crossed the midline and colonized the contralateral side much less frequently than did their wild-type counterparts (Table 1). Midline crossing between wild-type grafts and those of Type 1 *VEGF-A*$^{-/-}$ grafts that have roughly equivalent numbers of graft-derived endothelial cells and extensive migration were compared. Mutant endothelial cells were found on the contralateral side 13% of the time (1 of 8), whereas wild-type endothelial cells were found on the contralateral side 35% of the time (6 of 17). Thus, Type 1 *VEGF-A*$^{-/-}$ ES cell-derived endothelial cells/progenitors more closely resemble presomitic mesoderm-derived endothelial cells that never cross the host embryonic midline (0 of 17; Ambler et al., 2001). This result suggests that expression of VEGF-A by wild-type graft EBs can interfere with host midline patterning signals in a dominant manner, since abrogation of VEGF-A expression from the graft cells restores proper signaling at the host embryonic midline.

## Discussion

Our data strongly support a model of vascular patterning in which instructive spatiotemporal information is provided by signals from the embryonic environment (Fig. 8). In this model, the target angioblasts and endothelial cells are made competent to respond to these cues by the expression of receptors, including the VEGF receptor flk-1. This require-

ment suggests that one or more flk-1 ligands contribute to the host vascular patterning signals. The data supporting this model are: (1) both somite-derived and ES cell-derived endothelial cells/progenitors pattern similarly when placed in the presomitic mesoderm cavity of an avian host; (2) expression of the VEGF receptor flk-1 on target cells is required for proper migration and patterning; and (3) VEGF-A expression by target cells is not essential, and in fact, ectopic expression of VEGF-A by graft cells interferes with normal patterning at the embryonic midline. This model provides a framework for further dissection of vascular patterning information, and it has implications for therapeutic approaches to vascular disease.

The remarkable similarity between the patterning behavior of mouse somite-derived and ES cell-derived endothelial cells/progenitors (Ambler et al., 2001; and this work) strongly indicates that embryonic vascular cells from different sources mature through a similar stage where they are competent to respond to most environmental patterning cues. Alternatively, angioblasts from different sources could have different intrinsic developmental programs that specify responses to different subsets of vascular patterning cues. Since ES cells are totipotent, they may be unique in their ability to respond to a wider range of patterning cues than endothelial cells/progenitors derived from specific embryonic locations. However, grafts from different tissues placed heterotopically in quail-chick chimeras provide migratory angioblasts that form vessels (Noden, 1989; Poole and Coffin, 1989; Wilms et al., 1991; Pardanaud et al., 1996). Also, we have anecdotally noted that mouse somite grafts placed ectopically into mouse hosts form vessels in places where host vessels are predicted to form (V.L.B., unpublished results). These findings support the hypothesis that angioblasts from diverse locations can be made competent to respond to local vascular patterning cues.

Vascular patterning signals are likely to emanate from several embryonic structures. The consistent colonization of host vascular beds in the kidney, limb, perineural, and intersomitic areas by graft-derived vascular cells (Ambler et al., 2001; and this work) suggests that local vascular patterning cues are associated with structures in these areas, such as the neural tube and the limb. What could these patterning signals be? The inability of *flk-1*$^{-/-}$ graft cells to migrate and pattern in the avian host suggests that a ligand of this receptor is a critical component of one or more vascular patterning signals. VEGF-A, VEGF-C, and VEGF-D are flk-1 ligands that could provide patterning information in vivo (reviewed in Ferrara and Davis-Smyth, 1997). The expression patterns of all three ligands in avian embryos support a possible role in vascular patterning around the axial midline: VEGF-A is expressed in the neural tube and somites, VEGF-C is expressed in the kidney rudiment and myotome, and VEGF-D is expressed in the medial sclerotome (Aitkenhead et al., 1998; Eichmann et al., 1998; Trelles et al., 2002). Further support for the involvement of VEGF-A in patterning vessels is its role in the skin and in the retina (Stone et al., 1995; Mukuoyama et al., 2002). In these studies, the effects of VEGF-A were local and selectively affected the patterning of arteries. In contrast, VEGF-A appears to provide a long-range signal in Xenopus and zebrafish to pattern the dorsal aorta at the midline (Cleaver and Krieg, 1998; Liang et al., 2001). It will be interesting to determine how VEGF-A acts in vascular pattern formation around the mammalian axial midline.

One caveat to the interpretation that flk-1 is required for endothelial cells/progenitors to respond to vascular patterning cues is that nonpatterning aspects of vascular development are also compromised in the absence of flk-1. *Flk-1*$^{-/-}$ embryos and EBs make very few endothelial cells and blood vessels. However, several lines of evidence indicate that flk-1 is not absolutely required for angioblast differentiation. Initial formation of some vessels is seen in *flk-1*$^{-/-}$ mouse EBs and embryos, and zebrafish embryos lacking flk-1 make many vessels but have defects in angiogenic sprouting (Shalaby et al., 1995, 1997; Schuh et al., 1999; Habeck et al., 2002). Moreover, the *flk-1*$^{-/-}$ EBs and EB grafts in our study had reasonable numbers of cells that activated the flk-1 promoter (see Fig. 5A and B) and expressed PECAM (see Fig. 1D and Fig. 6A and B), both hallmarks of murine angioblasts. Thus, it is likely that at least a subset of angioblasts was available to respond to host patterning cues. However, we cannot formally rule out that flk-1 may be indirectly required for vascular patterning via a role in establishing angioblast competence to respond to vascular patterning signals. Conditional targeting strategies and site-directed mutagenesis of the flk-1 receptor are among the approaches that should clarify the role of flk-1 in vascular patterning responses.

In contrast to the cell-autonomous requirement for *flk-1*, VEGF-A expression by EB grafts is not required for proper migration and patterning of graft-derived vascular cells. EB grafts lacking VEGF-A (*VEGF-A*$^{-/-}$) produce endothelial cells/progenitors that migrate and pattern properly. This finding is consistent with a non-cell-autonomous role for VEGF-A in these processes that can be supplied by one or more host-derived factors. It is intriguing that small EBs (Type 1) produce vascular cells that pattern essentially like WT EB grafts, whereas larger EBs (Type 2) produce fewer vascular cells that pattern with lower frequency than WT EB grafts. It may be that host-derived vascular patterning signals are more accessible to angioblasts embedded in smaller EBs, while the larger EBs attenuate the effectiveness of host signals. Alternatively, the larger EBs may be more mature and their vascular cells may be less responsive to host-derived vascular patterning signals. These effects would not be obvious in wild-type EBs that produce VEGF-A throughout differentiation. Both scenarios suggest that there may be spatial restrictions on the effectiveness of signals, and/or temporal windows of angioblast competence to respond to vascular patterning signals. The identity of the

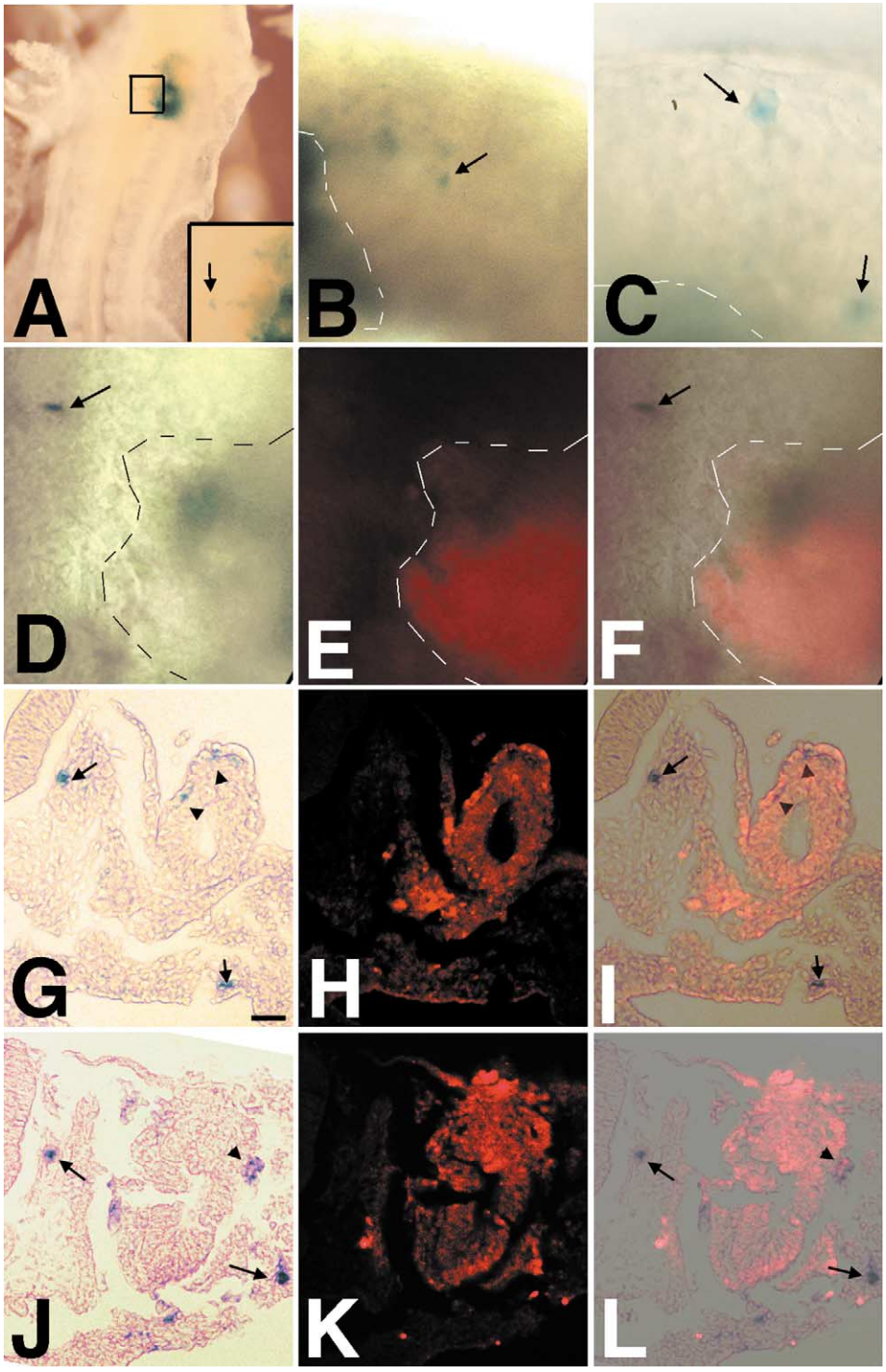


Fig. 5. Flk-1$^{+}$ graft-derived EB cells localize outside grafts at early time points. *Flk-1*$^{+/-}$ EBs were labeled with CM-DiI (red) before implantation into a quail host. Chimeric embryos were fixed at 18 (A), 24 (B, D–L), or 36 h (C) postsurgery and reacted for $\beta$-gal (blue). (A–F) Whole mounts. (G–L) Transverse sections. (A) EB graft, showing placement in the somitic area of the avian host. Day 3 EBs were placed into a 12-somite (HH stage 11−) host, and incubated for 18 h, to HH stage 17. The inset shows a higher magnification of the area adjacent to the graft, and the arrow indicates $\beta$-gal$^{+}$ cells that appear outside the putative perimeter of graft. (B) EB graft, showing $\beta$-gal$^{+}$ cells that appear outside the putative graft perimeter (white dashed line). Day 3 EBs were placed into a 19-somite (HH stage 13) host, and incubated for 24 h, to HH stage 20. The arrow indicates $\beta$-gal$^{+}$ cells that appear outside the putative graft perimeter. (C) EB graft, showing $\beta$-gal$^{+}$ cells that appear outside the putative graft perimeter (white dashed line). Day 3 EBs were placed into a 19-somite (HH stage 13) host, and incubated for 36 h, to HH stage 21. The arrows indicate $\beta$-gal$^{+}$ cells that appear outside the putative graft perimeter. (D–F) EB graft after 24 h. Day 3 EBs were placed into a 19-somite (HH stage 13) host, and incubated for 24 h, to HH stage 20. (D) Brightfield image. (E) Epifluorescence. (F) Merged view. Dashed line denotes EB graft perimeter, and the arrows in (D) and (F) indicate $\beta$-gal$^{+}$ cells outside the graft perimeter. (G–L) Transverse sections of chimeric embryos 24 h postsurgery viewed in bright field (G, J), epifluorescence (H, K), or merged (I, L). In (G), (I), (J), and (L), the arrows mark $\beta$-gal$^{+}$ cells outside the graft perimeter, and the arrowheads mark $\beta$-gal$^{+}$ cells inside the graft perimeter. Scale bar, 20 $\mu$m.

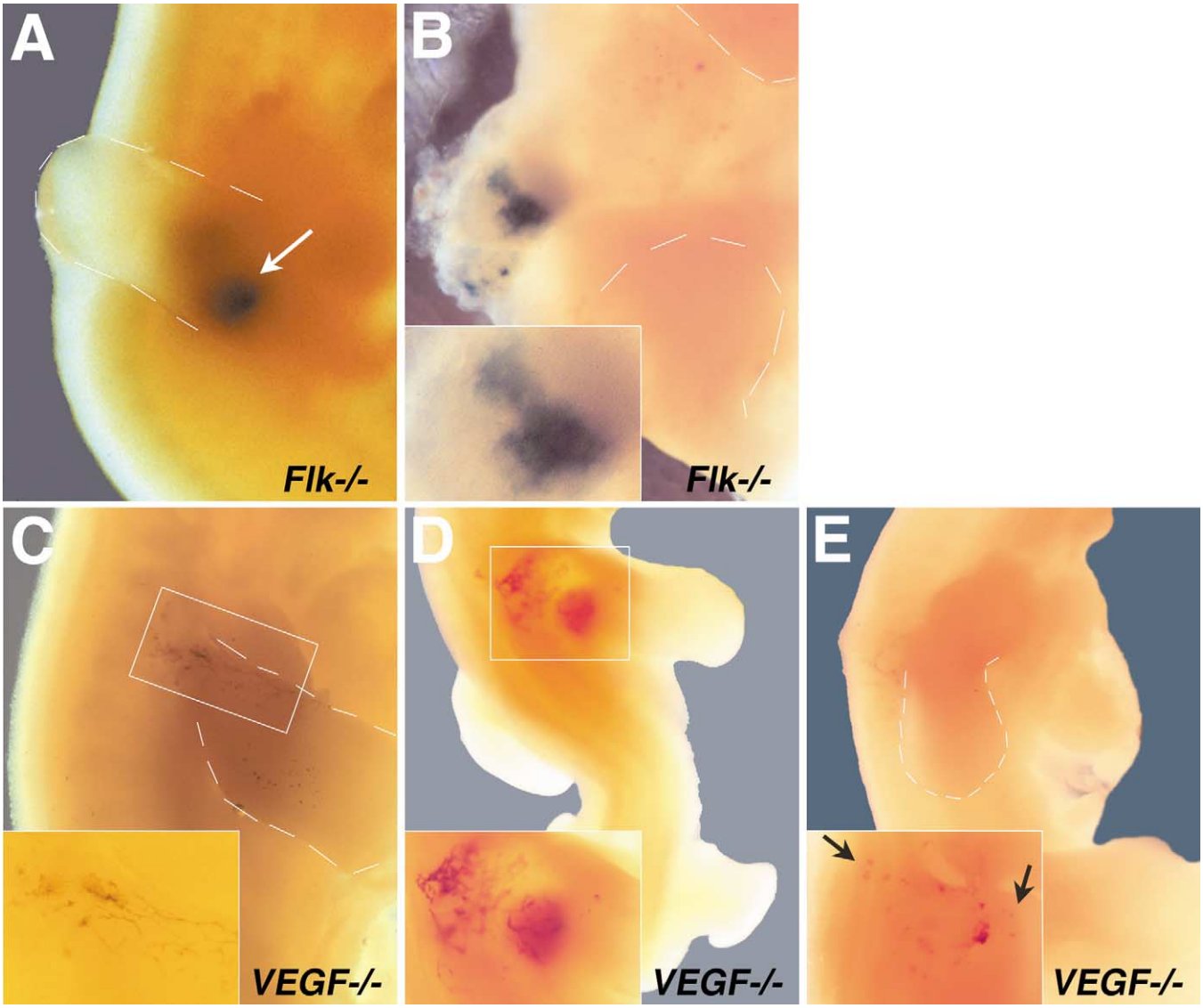


Fig. 6. Mutant EB grafts display both cell-autonomous and non-cell-autonomous patterning defects in avian hosts. EB–avian chimeras made with either *flk-1*$^{-/-}$ (A, B) or *VEGF-A*$^{-/-}$ (C–E) EBs were whole-mount stained for β-gal (blue) reactivity (A, B) or with PECAM (brown) (C–E) to visualize graft-derived vascular cells. (A, B) Two different examples of *flk*$^{-/-}$ grafts showing graft-derived cells that express β-gal from the flk-1 promoter but do not migrate extensively. Dashed lines outline the limb in each panel. (A) Day 4 EBs were placed into a 15-somite (HH stage 12−) host, and incubated for 3 days, to HH stage 24. The arrow points to β-gal-positive graft cells embedded within the chimeric embryo. (B) Day 4 EBs were placed into a 17-somite (HH stage 12+) host, and incubated for 3 days, to HH stage 24. The inset shows a higher magnification of the graft site. (C, D) Two different examples of *VEGF*$^{-/-}$ Type 1 grafts showing extensive dispersal of graft-derived vascular cells. In both cases, day 4 EBs were placed into a 14-somite (HH stage 11+) host, and incubated for 3 days, to HH stage 24. The dashed lines in (C) outline the limb. The boxed areas of each panel are shown at higher magnification in the insets, which show the extensive graft-derived vasculature. (E) An example of a *VEGF*$^{-/-}$ Type 2 graft showing some dispersal of graft-derived vascular cells that remain in small clumps. Day 4 EBs were placed into a 12-somite (HH stage 11−) host, and incubated for 3 days, to HH stage 24. The inset shows a higher magnification of the same graft, and the arrows point to small clumps of PECAM$^{+}$ angioblasts.

host-derived signals that rescue ES cell-derived vascular patterning is not formally known, but it is likely that avian VEGF family members contribute to this rescue.

The patterning of vascular endothelial cells relative to the embryonic midline is an interesting and somewhat mysterious process. Analysis of quail-chick chimeras shows that somite-derived avian endothelial cells do not cross the embryonic midline to colonize the contralateral side of the host, except when the notochord is removed (Wilting et al., 1995; Klessinger and Christ, 1996; Pardanaud et al., 1996). We have recently extended these results to mouse endothelial cells using mouse-avian chimeras (Ambler et al., 2001; and C.A.A. and V.L.B., unpublished results). Thus, the embryonic midline, which is established at gastrulation, maintains a barrier to endothelial cell crossing that requires an intact notochord for maintenance. We were initially quite surprised to find that ES cell-derived endothelial cells/progenitors derived from EB grafts crossed the host midline

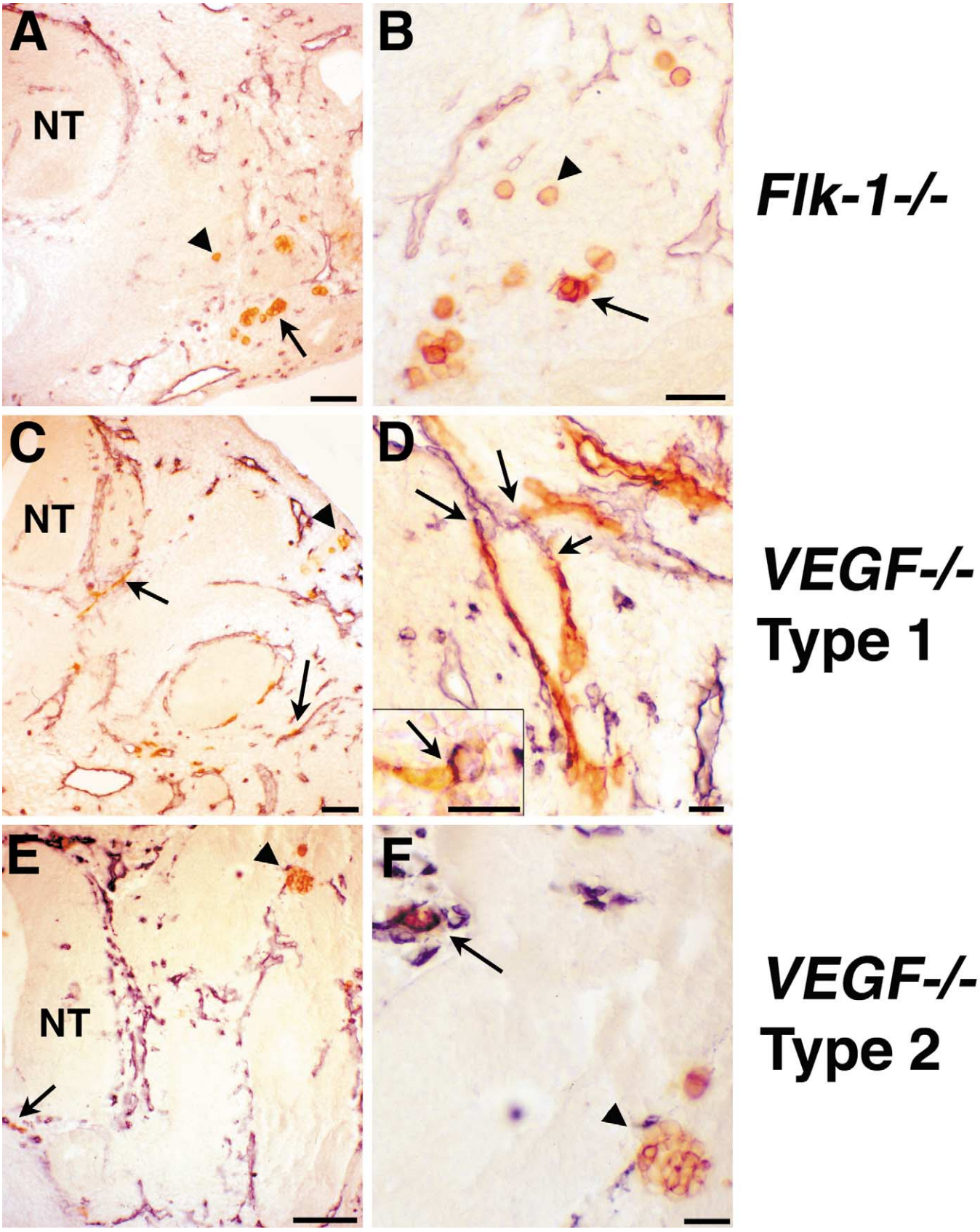


Fig. 7. Mutant ES cell-derived endothelial cells display both cell-autonomous and non-cell-autonomous patterning defects in avian hosts. EB–avian chimeras made with either *flk-1*$^{-/-}$ (A, B) or *VEGF-A*$^{-/-}$ (C–F) mutant EBs were whole-mount stained for PECAM (brown) reactivity to visualize graft-derived vascular cells, and transverse sections were then counterstained with QH1 (purple) to visualize host blood vessels. (A, B) Different areas of a *Flk*$^{-/-}$ graft

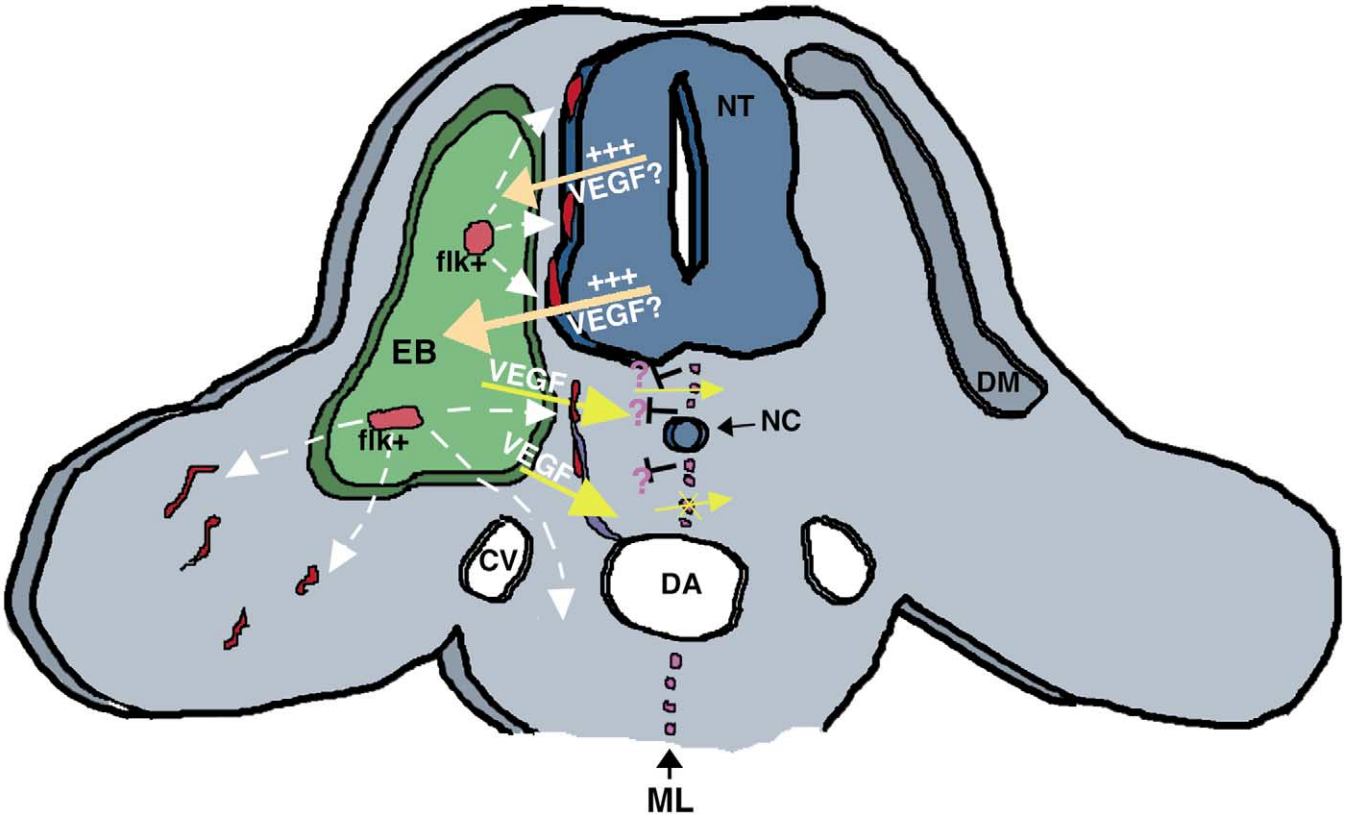


Fig. 8. Model of patterning interactions in EB–avian chimeric embryos. Schematic of a transverse section of an EB–avian chimera showing the migration and colonization patterns of ES cell-derived endothelial cells/progenitors in avian hosts. It also depicts one possible molecular scenario that is consistent with the data. The host neural tube produces a positive vascular patterning signal (orange arrows, VEGF?), and this signal acts on ES-cell derived endothelial/progenitors that express the VEGF receptor flk-1 (red cells, flk-1$^{+}$) to promote migration and patterning (dashed white arrows). At the same time, a restrictive vascular patterning signal emanates from the host midline (black stop lines, pink question marks) and prevents midline crossing of vascular cells. This signal, however, can be compromised by ectopic VEGF-A expression (yellow arrows, VEGF) so that endothelial cells/progenitors can cross the vascular midline (yellow X at midline). CV, cardinal vein; DA, dorsal aorta; DM, dermamyotome; EB, embryoid body; ML, midline; NC, notochord; NT, neural tube.

significantly more often than did somitic mesoderm-derived endothelial cells/progenitors (see Table 1). This result suggested that either ES cell-derived endothelial cells/progenitors differed from embryonic endothelial cells/progenitors in their ability to sense and respond to the midline barrier or that the host midline had been compromised.

The latter hypothesis is supported by our finding that ES cell-derived endothelial cells/progenitors from *VEGF-A*$^{-/-}$ EBs respected the midline barrier much more faithfully than did their wild-type counterparts. While this result does not formally rule out a cell-autonomous role for *VEGF-A* in midline sensing or barrier crossing, it is most consistent with a model in which VEGF-A signaling from nonendothelial cells in the EB graft disrupts the host midline and allows for midline crossing of graft cells (Fig. 8). Among the cell types that form during EB formation is visceral endoderm that is a potent source of VEGF-A expression (Keller et al., 1993; Leahy et al., 1999). This layer forms the outer layer of the EBs, analogous to its position in the yolk sac, and thus it would likely be the outermost layer of the EB grafts in avian hosts. From this position, VEGF-A could be secreted and diffuse to the host midline, where it may

showing small clumps of graft-derived angioblasts independent of host vessels. Day 4 EBs were placed into an 11-somite (HH stage 10+) host, and incubated for 3 days, to HH stage 24. The arrows point to small aggregates of angioblasts and arrowheads point to individual cells. Note the rounded morphology of the PECAM$^{+}$ angioblasts. (C, D) Different areas of a *VEGF*$^{-/-}$ Type 1 graft showing extensive dispersal of graft-derived vascular cells, and placement in vascular beds with host vessels. Day 4 EBs were placed into a 14-somite (HH stage 11+) host, and incubated for 3 days, to HH stage 24. The arrows in (C) point to examples of areas where graft-derived endothelial cells are closely apposed to host vessels, and the arrowhead points to a small clump of graft-derived angioblasts. The arrows in (D) point to examples of putative junctions between graft and host endothelial cells to make mosaic vessels. The inset shows a higher magnification of such a junction. (E, F) *VEGF*$^{-/-}$ Type 2 graft showing some dispersal of graft-derived vascular cells that generally are found in small clumps. Day 4 EBs were placed into a 14-somite (HH stage 11+) host, and incubated for 3 days, to HH stage 24. The arrows in (E) and (F) point to rare areas where graft-derived endothelial cells appear to form a mosaic vessel, and the arrowheads in each panel point to a clump of graft-derived angioblasts. NT, neural tube. Scale bars (A, C, E) = 40 $\mu$m; and (B, D, F and inset D) = 10 $\mu$m.

disrupt the barrier and/or the ability of endothelial cells/progenitors to sense the barrier. These findings do not rigorously demonstrate a requirement for VEGF-A in midline barrier function, but they show that VEGF-A can disrupt the barrier in a dominant fashion. However, the cell-autonomous requirement for flk-1 in vascular patterning coupled with these results suggests that VEGF-A may be involved in establishing and/or maintaining the midline barrier. Further experimentation combining genetic reagents and embryological techniques should resolve some of these unanswered questions.

In any case, the ability of ES cell-derived angioblasts and endothelial cells to respond to local vascular patterning cues suggests therapeutic approaches using stem cell-derived endothelial cells. Recent work shows that ES-cell derived endothelial cells can colonize host vessels when directly injected into the heart, and that ES cell-derived endothelial cells form vessels in tumors when coinjected with tumor cells (Yamashita et al., 2000; Marchetti et al., 2002). However, these studies did not address the patterning potential of ES cell-derived angioblasts. Our work suggests that, if a source of angioblasts were placed near a potential vascularization site in vivo, the vascular patterning cues intrinsic to the local environment might instruct the proper homing and patterning of the therapeutic angioblasts. Conversely, disruption of local vascular patterning cues may disrupt the surrounding vasculature and prevent proper vascular patterning. This scenario is supported by recent work showing that ectopic delivery of VEGF disrupts vessel blood formation in the local environment (Springer et al., 2000). Thus, EB–avian chimeric embryos will be useful to further test models of embryonic vascular patterning pathways, and these pathways are likely to be important in therapeutic vascularization as well. It should also provide a relatively efficient way to test a subset of the numerous mutations that have been generated in ES cells for their effect on vascular patterning.

## Acknowledgments

We thank Guo-Hua Fong, Janet Rossant, and Elizabeth Robertson for the *flt-1*+/−, *flk-1*−/−, and *ROSA26*+/− ES cells, respectively. We thank members of the Bautch Lab for fruitful discussions and an anonymous reviewer for cogent comments, and Susan Whitfield for artwork and photography. The QH1 monoclonal antibody developed by F. Dieterlen-Lievre was obtained from the Developmental Studies Hybridoma Bank under the auspices of the NICHD and maintained by The University of Iowa, Department of Biological Sciences, Iowa City, IA. The work was supported by a grant from the NIH (HL43174) to V.L.B. G.M.S. received a James Henley Thompson and Evelyn Barnett Thompson Undergraduate Research Award.

## References

Aitkenhead, M., Christ, B., Eichmann, A., Feucht, M., Wilson, D.J., Wilting, J., 1998. Paracrine and autocrine regulation of vascular endothelial growth factor during tissue differentiation in the quail. Dev. Dyn. 212, 1–13.

Ambler, C.A., Nowicki, J.L., Burke, A.C., Bautch, V.L., 2001. Assembly of trunk and limb blood vessels involves extensive migration and vasculogenesis of somite-derived angioblasts. Dev. Biol. 234, 352–364.

Baldwin, H.S., Shen, H.M., Yan, H.C., DeLisser, H.M., Chung, A., Mickanin, C., Trask, T., Kirschbaum, N.E., Neuman, P.J., Albelda, S.M., Buck, C.A., 1994. Platelet endothelial cell adhesion molecule-1 (PECAM/CD31): alternatively spliced, functionally distinct isoforms expressed during mammalian cardiovascular development. Development 120, 2539–2553.

Bautch, V. L., 2002. Turksen, K. (Ed.), Embryonic stem cell differentiation and the vascular lineage, in: Embryonic Stem Cells: Methods and Protocols, Humana Press, Totowa, NJ, pp. 117–125.

Bautch, V.L., Redick, S.D., Scalia, A., Harmaty, M., Carmeliet, P., Rapoport, R., 2000. Characterization of the vasculogenic block in the absence of vascular endothelial growth factor-A. Blood 95, 1979–1987.

Beddington, R.S.P., Morgernstern, J., Land, H., Hogan, A., 1989. An *in situ* transgenic enzyme marker for the midgestation mouse embryo and the visualization of inner cell mass clones during early organogenesis. Development 106, 37–46.

Childs, S., Chen, J.-N., Garrity, D.M., Fishman, M.C., 2002. Patterning of angiogenesis in the zebrafish embryo. Development 129, 973–982.

Clark, E.R., Clark, E.L., 1939. Microscopic observations on the growth of blood capillaries in the living mammal. Am. J. Anat. 64, 251–299.

Cleaver, O., Krieg, P.A., 1998. VEGF mediates angioblast migration during development of the dorsal aorta in Xenopus. Development 125, 3905–3914.

Daniel, T.O., Abrahamson, D., 2000. Endothelial signal integration in vascular assembly. Annu. Rev. Physiol. 62, 649–671.

Dent, J.A., Polson, A.G., Klymkowsky, M.W., 1989. A whole-mount immunocytochemical analysis of the expression of the intermediate filament protein vimentin in Xenopus. Development 105, 61–74.

Drake, C.J., Hungerford, J.E., Little, C.D., 1998. Morphogenesis of the first blood vessels. in: Fleischmajer, R., Timpl, R., Werb, Z. (Eds.), Morphogenesis: Cellular Interactions. N. Y., Acad, Sci., New York, pp. 155–180.

Eichmann, A., Corbel, C., Jaffredo, T., Breant, C., Jouko, V., Kumar, V., Alitalo, K., Le Douarin, N.M., 1998. Avian VEGF-C: cloning, embryonic expression pattern and stimulation of the differentiation of VEGFR2-expressing endothelial cell precursors. Development 125, 743–752.

Ferrara, N., Davis-Smyth, T., 1997. The biology of vascular endothelial growth factor. Endocr. Rev. 18, 4–25.

Fong, G.-H., Rossant, J., Gertsenstein, M., Breitman, M.L., 1995. Role of the Flt-1 receptor tyrosine kinase in regulating the assembly of vascular endothelium. Nature 376, 66–70.

Fong, G.H., Klingensmith, J., Wood, C.R., Rossant, J., Breitman, M.L., 1996. Regulation of flt-1 expression during mouse embryogenesis suggests a role in the establishment of vascular endothelium. Dev. Dyn. 207, 1–10.

Fong, G.H., Zhang, L., Bryce, D.M., Peng, J., 1999. Increased hemangioblast commitment, not vascular disorganization, is the primary defect in flt-1 knock-out mice. Development 126, 3015–3025.

Graef, I.A., Chen, F., Chen, L., Kuo, A., Crabtree, G.R., 2001. Signals transduced by $Ca^{2+}$/calcineurin and NFATc3/c4 pattern the developing vasculature. Cell 105, 863–875.

Habeck, H., Odenthal, J., Walderich, B., Maischein, H.-M., Tubingen 2000 screen consortium and Schulte-Merker, S. 2002. Analysis of a zebrafish

VEGF receptor mutant reveals specific disruption of angiogenesis. Curr. Biol. 12, 1405–1412.
Hamburger, V., Hamilton, H.L., 1951. A series of normal stages in the development of the chick embryo. J. Morphol. 88, 49–92.
Hogan, B.L.M., Kolodziej, P.A., 2002. Molecular mechanisms of tubulogenesis. Nat. Rev. Genet. 3, 513–523.
Kearney, J.B., Ambler, C.A., Monaco, K.A., Johnson, N., Rapoport, R.G., Bautch, V.L., 2002. Vascular endothelial growth factor receptor Flt-1 negatively regulates developmental blood vessel formation by modulating endothelial cell division. Blood 99, 2397–2407.
Keller, G., Kennedy, M., Papayannopoulou, T., Wiles, M., 1993. Hematopoietic commitment during embryonic stem cell differentiation in culture. Mol. Cell. Biol. 13, 473–486.
Klessinger, S., Christ, B., 1996. Axial structures control laterality in the distribution pattern of endothelial cells. Anat. Embryol. 193, 319–330.
Leahy, A., Xiong, J.-W., Kuhnert, F., Stuhlmann, H., 1999. Use of developmental marker genes to define temporal and spatial patterns of differentiation during embryoid body formation. J. Exp. Zool. 284, 67–81.
Liang, D., Chang, J.R., Chin, A.J., Smith, A., Kelly, C., Weinberg, E.S., Ge, R., 2001. The role of vascular endothelial growth factor (VEGF) in vasculogenesis, angiogenesis, and hematopoiesis in zebrafish development. Mech. Dev. 108, 29–43.
Marchetti, S., Gimond, C., Iljin, K., Bourcier, C., Alitalo, K., Pouyssegur, J., Pages, G., 2002. Endothelial cells genetically selected from differentiating mouse embryonic stem cells incorporate at sites of neovascularization in vivo. J. Cell Sci. 115, 2075–2085.
Mukuoyama, Y., Shin, D., Britsch, S., Taniguchi, M., Anderson, D.J., 2002. Sensory nerves determine the pattern of arterial differentiation and blood vessel branching in the skin. Cell 109, 693–705.
Noden, D.M., 1989. Embryonic origins and assembly of blood vessels. Am. Rev. Respir. Dis. 140, 1097–1103.
Orlidge, A., D'Amore, P.A., 1987. Inhibition of capillary endothelial cell growth by pericytes and smooth muscle cells. J. Cell Biol. 105, 1455–1462.
Otani, A., Kinder, K., Ewalt, K., Otero, F.J., Schimmel, P., Friedlander, M., 2002. Bone marrow-derived stem cells target retinal astrocytes and can promote or inhibit retinal angiogenesis. Nat. Med. 8, 1004–1010.
Pardanaud, L., Altmann, C., Kitos, P., Dieterlen-Lievre, F., Buck, C.A., 1987. Vasculogenesis in the early quail blastodisc as studied with a monoclonal antibody recognizing endothelial cells. Development 100, 339–349.
Pardanaud, L., Luton, D., Prigent, M., Bourcheix, L.-M., Catala, M., Dieterlen-Lievre, F., 1996. Two distinct endothelial lineages in ontogeny, one of them related to hemopoiesis. Development 122, 1363–1371.
Pereria, F.A., Qiu, Y., Zhou, G., Tsai, M.-J., Tsai, S. Y., 1999. The orphan nuclear receptor COUP-TFII is required for angiogenesis and heart development. Genes Dev. 13, 1037–1049.
Poole, T.J., Coffin, D., 1989. Vasculogenesis and angiogenesis: two distinct morphogenetic mechanisms establish embryonic vascular pattern. J. Exp. Zool. 251, 224–231.
Redick, S.D., Bautch, V.L., 1999. Developmental platelet endothelial cell adhesion molecule expression suggests multiple roles for a vascular adhesion molecule. Am. J. Pathol. 154, 1137–1147.
Risau, W., 1997. Mechanisms of angiogenesis. Nature 386, 671–674.
Sabin, F.R., 1917. Origin and development of the primitive vessels of the chick and of the pig. Contrib. Embryol. Carnegie Inst. 6, 61–124.
Schuh, A.C., Faloon, P., Hu, Q.-L., Bhimani, M., Choi, K., 1999. In vitro hematopoietic and endothelial potential of *flk-1*$^{-/-}$ embryonic stem cells and embryos. Proc. Natl. Acad. Sci. USA 96, 2159–2164.
Shalaby, F., Ho, J., Stanford, W.L., Fischer, K.-D., Schuh, A.C., Schwartz, L., Bernstein, A., Rossant, J., 1997. A requirement for Flk1 in primitive and definitive hematopoiesis and vasculogenesis. Cell 89, 981–990.
Shalaby, F., Rossant, J., Yamaguchi, T., Gertsenstein, M., Wu, X.-F., Breitman, M.L., Schuh, A.C., 1995. Failure of blood-island formation and vasculogenesis in Flk-1- deficient mice. Nature 376, 62–66.
Springer, M.L., Hortelano, G., Bouley, D.M., Wong, J., Kraft, P.E., Blau, H.M., 2000. Induction of angiogenesis by implantation of encapsulated primary myoblasts expressing vascular endothelial growth factor. J. Gene Med. 2, 279–288.
Stone, J., Itin, A., Alon, T., Pe'er, J., Gnessin, H., Chan-Ling, T., Keshet, E., 1995. Development of retinal vasculature is mediated by hypoxia-induced vascular endothelial growth factor (VEGF) expression by neuroglia. J. Neurosci. 15, 4738–4747.
Trelles, R.D., Leon, J.R., Kawakami, Y., Simoes, S., Izpisua-Belmonte, J.C., 2002. Expression of the chick *vascular endothelial growth factor D* gene during limb development. Mech. Dev. 116, 239–242.
Vittet, D., Prandini, M.H., Berthier, R., Schweitzer, A., Martin-Sisteron, H., Uzan, G., Dejana, E., 1996. Embryonic stem cells differentiate in vitro to endothelial cells through successive maturation steps. Blood 88, 3424–3431.
Wang, R., Clark, R., Bautch, V.L., 1992. Embryonic stem cell-derived cystic embryoid bodies form vascular channels: an in vitro model of blood vessel development. Development 114, 303–316.
Wilms, P., Christ, B., Wilting, J., Wachtler, F., 1991. Distribution and migration of angiogenic cells from grafted avascular intraembryonic mesoderm. Anat. Embryol. 183, 371–377.
Wilting, J., Brand-Saberi, B., Huang, R., Zhi, Q., Kontges, G., Ordahl, C.P., Christ, B., 1995. Angiogenic potential of the avian somite. Dev. Dyn. 202, 165–171.
Yamashita, J., Itoh, H., Hirashima, M., Ogawa, M., Nishikawa, S., Yurugi, T., Naito, M., Nakao, K., Nishikawa, S.-I., 2000. Flk-1 positive cells derived from embryonic stem cells serve as vascular progenitors. Nature 408, 92–96.
Zhang, Y., Porat, R.M., Alon, T., Keshet, E., Stone, J., 1999. Tissue oxygen levels control astrocyte movement and differentiation in developing retina. Dev. Brain Res. 118, 135–145.
Zhong, T.P., Rosenberg, M., Mohideen, M.-A.P.K., Weinstein, B., Fishman, M.C., 2000. Gridlock, an HLH gene required for assembly of the aorta in zebrafish. Science 287, 1820–1824.